Silicon-Integrated Uncooled Infrared Detectors: Perspectives on Thin Films and Microstructures

V.R. MEHTA,[1,3] S. SHET,[1] N.M. RAVINDRA,[1] A.T. FIORY,[1] and M.P. LEPSELTER[2]

1.—Department of Physics, New Jersey Institute of Technology, Newark, NJ 07102. 2.—BTL Fellows, Inc., Summit, NJ 07901. 3—E-mail: vrm2@njit.edu

Uncooled infrared (IR) photodetectors for telecommunications, optical processor interconnects, and focal plane arrays are advantageously integrated into systems that are silicon based through advanced thin-film technologies. This paper reviews challenges of materials, microstructures, interfaces, and reactions of thin-film materials and technologies posed by such applications.

Key words: Photoreceivers, microbolometers, micro-electro-mechanical systems (MEMS), photovoltaics, photoconductors

INTRODUCTION

Technologies for silicon process integration of infrared (IR) detector systems are driven by pursuits of low cost and high performance that are required for commercial viability. The high device yields that are commonplace in standard silicon integrated circuit (IC) manufacture are very attractive when applied to fabricating optoelectronic components with comparably superior uniformity and yield.

Infrared photodetector technologies based on quantum detection in semiconductors or bolometric detection (thermoresistors, including transition-edge superconductors) have used cryogenic cooling by either Peltier effect or Joule–Thompson refrigeration for optimum low signal sensitivity at wavelengths beyond the near IR ($\lambda > 1.5$ μm). Schottky-barrier focal plane array detectors,[1] for example, have been developed for multiple wavelength imaging pyrometry systems for military and civilian applications.[2] Uncooled technologies with reduced photon sensitivity are also of value in systems requiring small physical dimensions, lightweight, reduced complexity, and low component cost.

Uncooled detectors (operating at ambient and near-ambient temperature, regulated and unregulated) based on silicon are considered in this paper. In telecommunications, IR detectors operating at optical fiber band passes at 1.3 μm and 1.55 μm are needed for photoreceivers and transreceivers. For massively parallel duplex data links, optical interconnects require small area and low power IR detector arrays operating at terabit/second system rates. Uncooled focal plane arrays are used to produce low-cost and lightweight IR cameras for night vision, security, motion sensing, law enforcement, thermal imaging, medical, machine vision, firefighting, inspection, forward-looking IR radar, transportation, unmanned airborne vehicles, rescue operations, meterology, and numerous other applications. Infrared detector technologies employ several principles, including photovoltaics, photoconductors, Si and Ge devices, microbolometers, pyroelectrics, and micromechanics. For high-speed mid-IR devices (e.g., 8–12 μm, $>10^{10}$ Hz), inter-sub-band transitions in quantum well IR photodetectors (QWIPs)[3] are operated at cryogenic temperatures to suppress dark current or uncooled with heterodyne or photovoltaic detection.[4] At longer wavelengths, IR camera technologies are being adapted to extend their sensitivities beyond the IR into the terahertz region for see-through object detection, security, and defense applications. This paper will briefly review the application areas of communications receivers and IR focal plane arrays from the perspective of meeting challenges posed by thin-film structures in IR detectors.

SILICONIZED PHOTONICS

A recent presentation of a roadmap for high-speed optical interconnects[5] has recognized that optical

(Received July 5, 2004; accepted December 2, 2004)

links, which are now being used between computers and between circuit boards within computers, are headed toward becoming commonplace for connections between ICs on circuit boards and possibly as interconnects among subsystems on an IC chip. Since low cost is a significant driving factor, the IR detector technology is desirably uncooled and based on silicon (rather than, e.g., InGaAs). Low cost discrete components are needed for optical communications and micro-optical interconnects. Personal computers, workstations, and servers provide significant market demand and place the speed of internal links on par with long-range optical communications. Large-scale monolithic integration of photonic and complementary metal-oxide-semiconductor (CMOS) electronics will enable electronic and photonic IC (EPIC) technology that is expected to lead to major performance advances.[6] An EPIC chip will require an IR detector that is combined with a silicon-based laser IR source[7] and integrated with other components such as modulators.[8] The motivation for considering photodetectors based on silicon are the implications of low materials and fabrication costs,[9] when compared to modules hybridized with, e.g., high-speed InP photodiodes. To be competitive, however, silicon-based photodetectors need to fulfill requirements of high speed and high quantum efficiency for the desired application.

Si Photodetectors

The operating wavelengths of certain silicon detectors described herein are intended to be compatible (or hybridized) with 850-nm GaAs/AlGaAs vertical cavity surface emitting lasers, which can be fabricated at low cost. Resonant cavity enhanced p-i-n photodetectors are one approach to achieve high quantum efficiency by compensating for low photon absorption in high mobility (high resistivity) silicon. Devices that use a distributed Bragg reflector (DBR) for optical confinement are being proposed, although constraints on the operating wavelength need to be considered. Such a structure was recently implemented as a vertical silicon photodetector built into a mesa structure in an epitaxial Si layer with a SiO_2/Si superlattice reflector on the opposite face.[10] Two SiO_2 periods were found to give sufficiently high reflectivity at resonant wavelengths, owing to large contrast in indices of refraction.[11] An in-line array of 12 Si photoreceivers for optical interconnects was fabricated and operated with 40% (internal) quantum efficiency at 10 GHz and at wavelength $\lambda = 860$ nm. Integration of the resonant cavity structure into a standard CMOS process flow could be challenging, as it requires special fabrication steps to form two buried SiO_2 layers in the silicon wafers and to grow device-quality epitaxial layer for the vertical p-i-n photodiodes.

Various silicon p-i-n detectors with lateral charge collection have recently been fabricated in silicon-on-insulator (SOI) wafers, a substrate that is compatible with very large scale integration (VLSI) high-speed circuits.[12,13] The buried oxide and surface antireflection coating can be used to form an optical resonant cavity (of Q that is lower than for a DBR). In one approach, a lateral p-i-n device with alternating n+ and p+ 0.5-μm fingers has been implemented in a conventional CMOS process.[12] The speed of the lateral p-i-n devices, which is limited by slow drift to the contacts of carriers generated deep below the surface, can be improved by locating the contacts near the buried SiO_2 layer. A p-i-n diode operating at 850 nm and integrated with a transimpedance amplifier was fabricated on high-resistivity SOI and shown to have an external quantum efficiency of 10% and data rates possibly up to 8 Gb/s.[12] The speed tradeoff is determined by an optical absorption depth, which is commonly about 2 μm. Speeds of 10 Gb/s at a bit error rate of 10^{-9} have been achieved in avalanche multiplication mode of a p-i-n diode with a responsivity of 0.32 A/W.[13]

An alternative lateral p-i-n approach uses deeply buried electrodes that are formed in 8-μm-deep and 0.4-μm-wide trenches.[14] The process is a modification of device isolation employed in embedded dynamic random access memory circuits. The etched trenches were filled with heavily n- or p-doped polycrystalline silicon (poly-Si) to form interdigitated contacts. The advantage of this approach is that the optical absorption and the carrier transit paths are mutually perpendicular, and thus decoupled, allowing one to optimize for high speed (6.5 Gb/s data rate) and high efficiency (68% at 845 nm). Parasitic capacitance between the trenched electrodes is an important design consideration for optimizing photoreceiver speed.

The above results thus provide several options for a silicon-based photodetector technology for communications. High-speed silicide/silicon Schottky-barrier detectors[15] can also be used for uncooled photodetectors with suitable choice of Schottky-barrier height[16] that optimizes the desirable internal photoemission collection sensitivity and suppresses undesirable thermionic emission dark current. Similar detector structures have been used for UV detectors of notable radiation hardness[17] and for microwave detectors.[18] The silicon phototransistor is another photonic device technology that remains to be fully explored for IR applications.[19]

Ge and SiGe Photodetectors

Growth of high-quality (e.g., low threading dislocation density) Ge films on Si wafers has opened up the possibility of low-cost Ge-based photodetectors for near-IR communications bands at 1.3 μm and 1.55 μm and high-resolution spectral imaging in the near IR (800 nm) to mid IR (1600 nm) with high quantum efficiencies. A strain-relaxed graded buffer layer of Ge-Si alloy or superlattice structure is grown on Si to compensate for the 4% greater lattice spacing of Ge, relative to Si. The processing conditions, film thicknesses, compositions, and growth temperatures are engineered in such a way as to

form misfit dislocations parallel to the buffer layer and to suppress propagation of threading dislocations into the active Ge device layer. This method of preparing virtual Ge substrates (with graded buffer layers grown at 740°C) was used to fabricate 1-μm-thick vertical p-i-n diodes in insulating Ge operating at 1300 nm and with a responsivity of 0.145 A/W.[20] NiGe alloy films grown by a self-aligned nickel silicidation process were used to make low-resistivity contacts to a Sb-doped n+ top layer and a B-doped p+ buried layer. Dark current and resistance capacitance (RC) time constant of the structure limit the device performance.

Growth of Ge directly on Si has conventionally been considered disadvantageous because of the islanding growth habit and dislocation formation. However, it was recently found that an ultra-high-vacuum chemical vapor deposition process from GH_4 precursor can be used to grow a sufficiently uniform Ge film at a deposition temperature of 380°C to suppress islanding and interfacial defects.[21] Lateral interdigitated finger contacts, 1-μm wide and spaced 2 μm apart, were formed using a 50-nm amorphous Ge (a-Ge) film under a 100-nm Ag contact. The higher mobility gap of a-Ge, relative to the band gap of Ge, is presumed to yield a Schottky-barrier height for Ag/a-Ge that is higher than for Ag/Ge, thus reducing the dark current by over 2 orders of magnitude to a manageable level (0.6 A/cm^2). Devices operating at 4.3 GHz have 14% external (43% internal) quantum efficiency and 0.15 A/W responsivity at 1300 nm.

Silicon-germanium technology has been introduced into high-speed CMOS technology to capture increased carrier mobility advantages of strained-layer epitaxy, which is 46% for n-channel devices and 60 to 80% for p-channel devices. Nanotechnology is implemented, for example, by finfet transistor designs that enable the manufacturability of aggressive high-performance design rules. Commercially viable integration of photoreceiver devices with SiGe CMOS needs to be attentive to compatible materials, thermal budget and processing requirements, and in particular to the inherent metastability of the semiconductor strained layers.[22]

Structures containing SiGe alloys and heterostructure bipolar transistors have potential applications as optical data links and optoelectronic ICs.[23] Strained superlattice structures comprising 30 alternating layers of 32-nm Si and $Si_{0.9}Ge_{0.1}$ alloy layers deposited on Si by selective epitaxial growth have been used for the active absorber region for a planar p-i-n photoreceiver.[24] The superlattice was formed in a planar silicon waveguide cladded by SiO_2 reflectors in a bonded SOI wafer. Infrared radiation at 980 nm was coupled into the device from a 125-μm diameter 10-μm core optical fiber set into a trench in the Si substrate abutting the Si waveguide. A device with GeSi absorber measuring 10 μm in width and 100 μm in length exhibited 25% external quantum efficiency. The frequency response at 3db bandwidth was found to be 10.5 GHz.

IR IMAGING

Infrared imaging in the midwavelength IR (e.g., 3–5 μm) and long-wavelength IR (e.g., 7–14 μm) with cooled detectors (or uncooled detectors with heterodyne detection) has been developed into an advanced art. This generally employs photonic detection methods using narrow band-gap semiconductors (InGaAs, HgCdTe, InSb, Ge) or Schottky-barrier detectors (PtSi/p-Si, Ir_2Si/p-Si) that are cryogenically cooled to suppress thermally emitted dark currents. The detectors are used as pixels in focal plane arrays for IR imaging systems, including multiwavelength thermal imaging and pyrometry. For example, focal plane arrays of QWIP detectors with electrical bias tuning to modulate IR response spectra have been proposed for multiple wavelength imaging systems.[25] The Ge detectors are in the borderline wavelength region and can be operated uncooled in some applications. The advantage of photonic detectors is the high efficiency detection of IR radiation in weak signal applications. A further advantage of cooling is suppression of noise from ambient radiation emitted by the apparatus.

Uncooled IR detectors circumvent the dark current issue by several approaches that can be broadly categorized as photoconductors and microbolometers. Photoconductors (e.g., PbS, PbSe, CuInSe, CdS, CdSe, Se, or Te) are used in the form of deposited films. Microbolometers detect IR radiation through the direct or indirect heating of a low-mass element that has a temperature-dependent physical property. Materials are fabricated as thin films that are supported by (or part of) thermally isolated membranes. Materials include thermistors with high-temperature coefficients of resistance (e.g, VO_x, a-Si, poly-SiGe, Ti, Nb, $YBa_2Cu_3O_6$); pyroelectrics with strong temperature-dependent dielectric polarization (e.g., $LiTaO_4$, $BaSrTiO_3$, $YBa_2Cu_3O_6$); silicon devices (e.g., Schottky-barrier diodes, transistors); thermoelectrics (e.g., BiSbTe, Si p-n junctions); and microcantilevers (e.g., bimaterial strips). Some nominally uncooled detector systems may require or benefit from temperature stabilization.

In the long-wave IR region, the IR sensitivity of uncooled detectors can approach that of cooled photonic detectors.

MICROBOLOMETERS

Focal plane arrays using microbolometer pixels for IR detection lend themselves to either direct integration with CMOS electronics or as a component in hybrid modules with separate read-out electronics.[26] A common procedure for making compact modules is to solder-bump mount the detector focal plane array with a Si IC chip. The CMOS integration compatibility involves pixel formation either embedded in a CMOS process or in the post-CMOS back end process. Thermal isolation of the pixel sensor is achieved by forming the detector element

on a membrane that is supported and thermally isolated by a microbridge structure. Fabrication of microbolometers uses micro-electro-mechanical systems (MEMS) process techniques.

The essentials of the microbolometer concept are shown in Fig. 1, where a resistor is suspended on a thin SiO_2 membrane web formed by selective etching.[27] In this structure, passive elements (resistors or capacitors) are decoupled from active devices in the Si substrate (transistors). The MEMS processing methods for fabricating microbolometer detectors were originally developed at Bell Labs for air-bridge isolation in ICs. A Schottky-barrier microbolometer sensor is illustrated by the circuit in Fig. 2.[28] The sensing element is a differential pair of PtSi/p-Si and RhSi/p-Si Schottky-barrier diodes that are formed on the SiO_2 membrane. The operating principle is the log-linear temperature dependence of Richardson thermionic emission currents in reverse-biased Schottky diodes. Thermionic Schottky-barrier devices have performance advantages over thermoresistive devices (e.g., VO_x films), owing to the absence of 1/f noise and low operating current.[29] The design in Fig. 2 has the further advantage in that it generates a thermodynamic output signal with a self-referencing zero offset. These attributes, combined with silicon-based device processing, yield intrinsic uniformity in contrast and gray scale of pixels in IR focal plane arrays. Air-bridge structures have wide application; for example, they are found in monolithic SiGe IR detectors.[24]

Microbolometer focal plane arrays for IR imaging may use either chopper or chopperless signal detection schemes. Capacitive sensors that are based on thermal dielectric response, e.g., $BaSrTiO_3$, are convenient for alternating current coupled detection. Thermoresistive film sensors such as VO_x and a-Si and thermoelectric film sensors (e.g., thermocouples containing poly-Si or doped Si) generally use direct current coupled detection. Typical performance of IR cameras based on these sensors achieves noise equivalent temperature differences and minimum resolvable object temperature differences below 0.03 K at f/1.0 optics. Ambient background radiation in uncooled systems ultimately determines that the noise sensitivity of microbolometers will be greater than for cooled photodetectors. Performance metrics

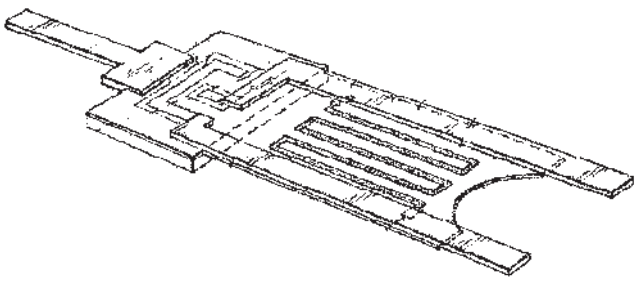

Fig. 1. Prototypical microbolometer structure with passive resistive element supported by a thin SiO_2 membrane to provide decoupling from active transistor (Ref. 27).

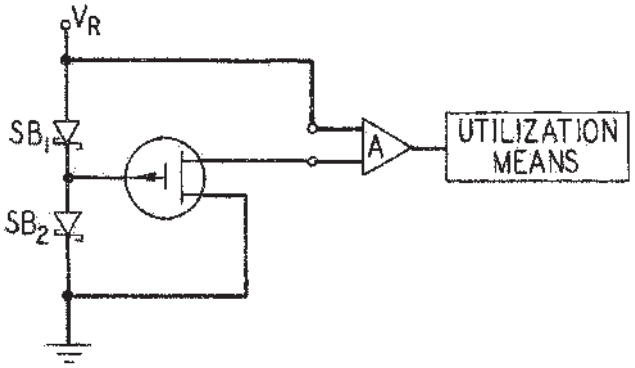

Fig. 2. Circuit for microbolometer IR detector with thermistor comprising two reverse-biased Schottky-barrier diodes of differing Schottky-barrier heights (Ref. 28).

comparing microbolometers and photodetectors have recently been reviewed.[30]

In general, detector selection considers thermal responsivity of the detector element, resolvable object temperature difference (ΔT) and response time (e.g., for 30 Hz framing rate). Pixel spacing for high-resolution imaging are as small as 20 μm. Operating wavelengths have been extended to 25 μm in applications for detecting concealed cold targets (e.g., under clothing).[31] Considerations for pixel type include materials, film stress, 1/f noise, mechanical noise, and internal thermal noise. A pixel with levitation of the detector element by electrostatic forces has been proposed for minimizing thermal conduction and for providing thermal quenching and baseline correction without the need for a chopper.[32]

Design and fabrication issues are uniformity, process control and integration, and pixel thermal cross talk. Focal plane array system requirements consider dynamic range, gray scale resolution, speed, read-out method (electronic, mechanical), gain and offset compensation, and signal leveling. Gain calibration (through hardware and software) relative to a uniform blackbody source is a crucial and painstaking task in setting up high-resolution, high-sensitivity IR cameras. Focal plane arrays with on-chip electronics can build in much of the interpixel leveling to achieve gray scale uniformity in the output electronic image.

DEPOSITED FILMS

Several new approaches have been reported for producing thin conductive films for microbolometer and photoconductor applications. Amorphous Si (a-Si) films are attractive for producing low-cost focal plane arrays.[33] Hydrogenated amorphous silicon films deposited by plasma-enhanced chemical vapor deposition on thin silicon nitride membranes are being used to form microbolometers for IR imaging (resonant quarter-wave pixel structures) and for multichannel gas sensing.[34] Deposited amorphous $Ge_xSi_{1-x}O_y$ films are also being investigated for resistive microbolometer sensors, owing to compatibility of the processing steps with IC fabrication.[35]

Thin vanadium suboxide (VO_x, where $x \approx 1.75$) films are commonly used as the resistive temperature sensor in microbolometers. Films with both low resistivity for low electrical noise and high fractional temperature coefficient of resistance (TCR) for high thermal sensitivity, arising from a variable-range hopping mechanism, are inherently unstable amorphous or mixed oxide composites. In a recent development, the desired mixed oxide phase was formed by rf sputter deposition of a three-layer precursor film structure comprising V_2O_5, V metal, and V_2O_5.[36] The deposited film stack is subsequently annealed in O_2 (30 min, 300°C) wherein the V reacts to form a mixed oxide phase layer (V_2O_3, VO_2, V_2O_5, etc.) sandwiched between two partially reduced V_2O_5 layers. With high TCR from the VO_2 and low film resistance from V_2O_5, the film exhibits a TCR of 2.5%/K and effective resistivity of 0.1 Ωcm. The process was used to make micromachined 50-μm pixels with 20-kΩ (~68-nm film thickness) VO_x films. Controlled oxidation of sputter-deposited V metal films in an O_2/Ar ambient at 300°C has also recently been advanced to produce VO_x films for microbolometer pixels with detectivity $D^* = 2 \times 10^8$ cmHz$^{1/2}$/W in CMOS compatible micromachining process.[37] These oxidation methods may have advantages over direct deposition from a mixed VO_x source material, such as by laser ablation.[38]

Lead chalcogenide photoconductors such as PbS and PbSe are noted for high detectivity and fast response in low-cost medium-wave IR detectors. The mechanism of photoconductivity in these materials is believed to involve generation of electron-hole pairs in microcrystals, thermally activated mobility (transport over intergrain barriers), and minimum conductivity. High photoconductivity response requires an oxidizing reaction in the film formation process. A low-temperature (350°C) method for producing an oxygen-sensitized PbSe:O film (0.5-μm microcrystal texture) was recently developed, which uses the reaction $PbI_2 + {}^1/_2Se \rightarrow PbSe + I_2$.[39] A film with Au contacts was integrated onto an IR filter (3–5μm) on a sapphire substrate to form a test structure. The films could be used in a multiwavelength system fabricated with silicon-compatible processes.

Semiconducting $YBa_2Cu_3O_{6+x}$ (YBCO) has a high TCR of 3–5%/K, making it an attractive material for a resistive microbolometer[40] as well as a pyroelectric film detector.[41] A resistive bolometer array was fabricated using a MEMS process where the YBCO was deposited on MgO buffer layer over a SiO_2 suspended membrane.[40] Responsivity of 560 V/W and $D^* \approx 10^7$ cmHz$^{1/2}$/W was recorded for broadband IR detection. The pyroelectric detector was made with YBCO film contacted with Nb electrodes and was supported by a SiO_2 film isolated by a trench in the Si substrate.

Deposition of YBCO on flexible substrates is being developed for such so-called smart skin applications as physiological monitoring and robotics where the detector needs to be foldable and wearable.[42] There are several process challenges to produce film structures that contain YBCO, Ti/Au contacts, and a Si_3N_4/polyimide cap. For direct deposition on a flexible substrate, such as a polyimide, maintaining the flatness of the substrate during processing requires depositions on both sides of the material to keep the film stress forces balanced. In an alternative spin-on process using MgO as a release layer on an oxidized Si holder wafer, the main challenge is reliably removing the film stack from the Si carrier (without curling). A device with a quarter-wave mirror comprising a multilayer of $Si_3N_4/LaAl_2O_3$/Al was fabricated having a TCR of 3%/K, responsivity of 3500 V/W, and $D^* = 10^7$ cmHz$^{1/2}$/W. Active device noise limits the D* in resistive YBCO microbolometers.

Pulsed laser deposition methods have been used to deposit films for microbolometer detectors. Films of $Ba_{0.7}5Sr_{0.25}TiO_3$ (BST) deposited at 520°C show the temperature coefficient of dielectric constant of 1%, which, while smaller than in the bulk crystal, is sufficient for $D^* = 1.6 \times 10^7$ cmHz$^{1/2}$/W in capacitively balanced and chopperless micromachined pixels.[43]

MICROMACHINED STRUCTURES

A number of innovations in silicon micromachined architectures have offered improved sensitivity of resistive microbolometers. A two-level microbridge and poststructure has been used to fabricate an IR microbolometer comprising a 50-nm Ti film sensor (TCR = 0.26%/K) on a silicon oxynitride membrane micromachined from a plasma-enhanced chemical-vapor-deposited film.[44] The multilevel structure reduces thermal cross talk between pixels and improves thermal isolation from the substrate while also maximizing the detector area (fill factor). The design was applied to produce pixels with a fill factor of 92%, response time of 12 ms, responsivity of 1600 V/W, and $D^* = 5 \times 10^8$ cmHz$^{1/2}$/W.

Antenna-coupled microbolometers have been used advantageously for fast response detection in the long-wave IR region.[45] In this method, IR radiation received by the antenna induces a current that in turn heats a thermally sensitive resistive element. Antennas have been shaped for resonance at a particular IR wavelength or narrow IR band, and to provide polarization sensitivity in the microbolometer method. E-beam lithography was used to fabricate log-periodic antenna arrays with Nb and VO_x sensing elements designed for IR imaging at 10 μm.[46] A similar method with reactive ion etching and liftoff was used to fabricate dipole antenna arrays with Nb film sensors.[47]

Conventional CMOS processing has been shown to be well suited for fabricating low-cost microbolometers in silicon. In a recent innovation, a Si n-well suspended by two arms was used to support an absorber film of poly-Si or an interconnect metal.[48] Poly-Si detectors show improved responsivity (2000 A/W), detectivity ($D^* = 2.6 \times 10^8$ cmHz$^{1/2}$/W), and noise equivalent detector temperature (NEDT = 0.2 K)

compared to earlier low-cost CMOS processes with thermoelectric-based detectors. A closed-loop version of the suspended n-well detector has been made with two P Metal Oxide Semiconductor (PMOS) devices, a thermistor and a controllable heat-balancing resistor (a transistor in saturation bias).[49] The device was suspended by oxide-coated poly-Si beams and coated with a metal film for visible light shielding. The control current supplied by an external simple cascode CMOS amplifier circuit with a temperature reference was used to produce the electrothermal readout signal. The detectivity in this design is limited to 10^8 $cmHz^{1/2}/W$ by active device noise.

Micro-optical–mechanical systems may hold promise for a direct optical readout IR camera. In one approach, the camera contains a focal plane array consisting of SiN_x/Au cantilevers with IR absorbing surfaces that deflect upon IR heating owing to differential thermal expansion.[50] A visible light source projected on the opposing faces of the cantilevers, which are reflective in the visible light, is focused on a video camera to produce an effective IR image (deflection resolution of 1 nm). The method is believed to have a noise equivalent temperature difference sensitivity of 0.03 K to 0.05 K. A more recent modification uses two pairs of bimaterial legs (Au/Si) to support the IR sensing vane to compensate for ambient heating and to provide self-leveling to the Si substrate.[51] The sensor in this case is a Pt/Si optical cavity with maximum sensitivities at 3.75 μm and 8.5 μm. The challenges in mechanical-based IR focal plane arrays lies in forming films with low mechanical stress, pixel uniformity, and mechanical noise suppression.

CONCLUSIONS

Low-cost and high-performance IR detector technologies are being developed for manufacture in silicon IC foundry and custom bolometer foundry facilities. Key performance metrics for silicon-integrated IR detector systems are speed and photonic sensitivity. The market drivers include massively parallel high-speed interconnects for communications, an all silicon-based optoelectronics, IR imaging systems that are easy to use and of low cost (e.g., less than $1,000), and weak IR signal applications requiring high photonic sensitivity. Challenges in thin films and microstructures are being addressed by using novel materials and film deposition strategies, and by adapting CMOS processes. Emulation of the CMOS IC foundry model is being pursued to achieve process yields and low manufacturing costs comparable to commodity ICs (e.g., routine 100% pixel yield in focal plane arrays with high resolution and pixel count). High-speed device architecture with Ge and SiGe integration is being used for 800- to 1,700-nm IR photodiode components and high-resolution focal plane arrays. Bolometer technologies have progressed to where they achieve resolvable object temperature differences and fast response comparable to photoelectric detectors in the long wavelength IR. Controlling film stress and process uniformity are common issues in the fabrication of IR focal plane arrays.

ACKNOWLEDGEMENTS

The authors acknowledge assistance from TMS, New Jersey Institute of Technology, Integron Solutions, BTL Fellows, and Lucent Technologies.

REFERENCES

1. Walter F. Kosonocky, *Review of Schottky-Barrier Imager Technology*, SPIE Advent Technologies Series, Vol. AT 2: Current Overviews in Optical Science and Engineering II, ed. Richard Feinberg (Bellingham, WA: SPIE, 1990), pp. 446-70.
2. W.F. Kosonocky, M.B. Kaplinsky, N.J. McCaffrey, E.S. Hou, C.N. Manikopoulos, N.M. Ravindra, S. Belikov, J. Li, and V. Patel, *Proc. SPIE* 2225, 26 (1994).
3. *Quantum Well Intersubband Transition Physics and Devices*, eds. H.C. Liu, B.F. Levine, and J.Y. Andersson (Dordrecht: Kluwer Academic, 1994).
4. H. Schneider, C. Schönbein, G. Bihlmann, P. van Son, and H. Sigg, *Appl. Phys. Lett.* 70, 1602 (1997).
5. N. Savage, *IEEE Spectrum* 39, 32 (2002).
6. U.S. Defense Advanced Research Projects Agency, *Electronic & Photonic Integrated Circuit (EPIC)*, http://www.darpa.mil/baa/baa04-15.htm (accessed June 9, 2004).
7. L Pavesi, *J. Phys.: Condens. Matter* 15, R1169 (2003).
8. A. Liu, R. Jones, L. Liao, D. Samara-Rubio, D. Rubin, O. Cohen, R. Nicolaescu, and M. Paniccia, *Nature* 427, 615 (2004).
9. A.T. Fiory and N.M. Ravindra, *J. Electron. Mater.* 92, 1043 (2003).
10. M.K. Emsley, O.I. Dosunmu, P. Muller, M.S. Ünlü, and Y. Leblebici, *Proc. SPIE Active and Passive Optical Components for WDM Communications III*, 5246, 409 (2003).
11. N.M. Ravindra, K. Ravindra, S. Mahendra, B. Sopori, and A.T. Fiory, *J. Electron. Mater.* 92, 1052 (2003).
12. S.M. Csutak, J.D. Schaub, W.E. Wu, and J.C. Campbell, *IEEE Photon. Technol. Lett.* 14, 516 (2002).
13. B. Yang, J.D. Schaub, S.M. Csutak, D.L. Rogers, and J.C. Campbell, *IEEE Photonics Technol. Lett.* 15, 745 (2003).
14. M. Yang, D.L. Rogers, J.D. Schaub, J.J. Welser, D.M. Kuchta, D.C. Boyd, F. Rodier, P.A. Rabidoux, J.T. Marsh, A.D. Ticknor, Q. Yang, A. Upham, and S.C. Ramac, *IEEE Electron. Dev. Lett.* 23, 395 (2002).
15. E. Chen and S.Y. Chou, *Appl. Phys. Lett.* 70, 753 (1997).
16. S.P. Murarka, *Silicides for VLSI Applications* (New York: Academic Press, 1983).
17. K. Solt, H. Melchior, U. Kroth, P. Kuschnerus, V. Persch, H. Rabus, M. Richter, and G. Ulm, *Appl. Phys. Lett.* 69, 3662 (1996).
18. Y. Wu, B.M. Armstrong, H.S. Gamble, Z. Hu, Q. Chen, S. Yang, V.F. Fusco, and J.A. Carson Stewart, *IEEE Trans. Microwave Theory and Techniques* 46, 641 (1998).
19. S.M. Sze, *Physics of Semiconductor Devices*, 2nd ed. (New York: John Wiley & Sons, 1981), ch. 13, pp. 743–790.
20. G. Wöhl, C. Parry, E. Kasper, M. Jutzi, and M. Berroth (Paper presented at 2003 IEEE Int. Solid State Circuits Conf., San Francisco, CA, 2003).
21. J. Oh, S.K. Banerjee, and J.C. Campbell, *IEEE Photonics Technol. Lett.* 16, 581 (2004).
22. A.T. Fiory, J.C. Bean, R. Hull, and S. Nakahara, *Phys. Rev. B* 31, 4063 (1985).
23. O. Qasaimeh, Z. Ma, P. Bhattacharya, and E.T. Croke, *J. Lightwave Technol.* 18, 1548 (2000).
24. T. Tashiro, T. Tatsumi, M. Sugiyama, T. Hashimoto, and T. Morikawa, *IEEE Trans. Electron. Dev.* 44, 545 (1997).
25. M. Mitra, U.S. patent application 2004/0108564 (10 June 2004); U.S. patent application 2004/0108461 (10 June 2004).
26. R.W. Wood, U.S. patent application 2003/0057371 (27 March 2003).
27. M.P. Lepselter, U.S. patent application 3,411,048 (Nov. 12, 1968).

28. J.M. Andrews and M.P. Lepselter, U. S. patent 3,719,797 (6 March 1973).
29. J.E. Murguia, P.K. Tedrow, F.D. Shepherd, D. Leahy, and M.M. Weeks, *SPIE* 3698, 361 (1999).
30. G. Sarusi, *Proc. SPIE* 4820, 919 (2003).
31. O.J. Milton, R.M. Walker, and R.W. McMillan, *Proc. SPIE* 4719, 167 (2002).
32. M.L. Reed and T.N. Blalock, U.S. patent application 2003/0141453 (31 July 2003).
33. A. Bain, J.L. Martin, and E. Mottin, *Sensor and Materials* 12, 365 (2000).
34. A.J. Syllaios, T.R. Schimert, R.W. Gooch, W.L. McCardel, B.A. Ritchey, and J.H. Tregilgas, *Mater. Res. Soc. Conf. Proc.* 609, A14.4.1-6 (2001); T.R. Schimert, N. Cunningham, G.L. Francisco, R.W. Gooch, J. Gooden, P. McCardel, B.E. Neal, B. Ritchey, J. Rife, A.J. Syllaios, J.H. Tregilgas, J.F. Brady III, J. Gilstrap, and S.J. Ropson, *Proc. SPIE* 4232, 187 (2001).
35. E. Iborra, M. Clement, L. V. Herrero, and J. Sangrador, *J. Microelectromech. Systems* 11, 322 (2002).
36. H.K. Kang, Y.g H. Han, H.J. Shin, S. Moon, and T.H. Kim, *J. Vac. Sci. Technol.* B 21, 1027 (2003).
37. H. Wang, X. Yi, G. Huang, J. Xiao, X. Li, and S. Chen, *Infrared Phys. Technol.* 45, 53 (2004).
38. R.T. Rajendra Kumar, B. Karunagaran, D. Mangalaraj, Sa. K. Narayandass, P. Manoravi, M. Joseph, and V. Gopal, *Smart Mater. Struct.* 12, 188 (2003).
39. J. Diezhandino, G. Vergara, G. Pérez, I. Génova, M.T. Rodrigo, F.J. Sánchez, M.C. Torquemada, V. Villamayor, J. Plaza, I. Catalán, R. Almazán, M. Verdú, P. Rodríguez, L. J. Gómez, and M.T. Montojo, *Appl. Phys. Lett.* 83, 2751 (2003).
40. C.M. Travers, A. Jahanzeb, D.P. Butler, and Z. Çelik-Butler, *J. Microelectromech. Systems* 6, 271 (1997).
41. A. Jahanzeb, C.M. Travers, D.P. Butler, Z. Çelik-Butler, and J.E. Gray, *Appl. Phys. Lett.* 70, 3495 (1997).
42. A. Yildiz, Z. Çelik-Butler, and D.P. Butler, *IEEE Sensors J.* 4, 112 (2004).
43. M. Noda, H.P. Xu, and T. Mukaigawa, *Sensor Mater.* 12, 375 (2000).
44. H.-K. Lee, J.-B. Yoon, E. Yoon, S.-B. Ju, Y.-J. Yong, W. Lee, and S.-G. Kim, *IEEE Trans. Electron. Dev.* 46, 1489 (1999).
45. I. Codreanu and G.D. Boreman, *Infrared Physics and Technology* 43, 335 (2002).
46. F.J. González, M. Abdel-Rahman, and G.D. Boreman, *Microwave and Optical Technol. Lett.* 38, 235 (2003).
47. M.A. Gritza, I. Puscasu, D. Spencer, and G.D. Boreman, *J. Vac. Sci. Technol. B* 21, 2608 (2003).
48. D.S. Tezcan, S. Eminoglu, and T. Akin, *IEEE Trans. Electron Dev.* 50, 494 (2003).
49. C.-C. Liu and C.H. Mastrangelo, *IEEE J. Solid State Circuits* 35, 527 (2000).
50. T. Perazzo, M. Mao, O. Kwon, A. Majumdara, J.B. Varesi, and P. Norton, *Appl. Phys. Lett.* 74, 3567 (1999).
51. J.L. Corbeil, N.V. Lavrik, and S. Rajic, P.G. Datskosa, *Appl. Phys. Lett.* 81, 1306 (2002).